HHS Public Access

Author manuscript

Exp Mol Pathol. Author manuscript; available in PMC 2024 December 05.

Published in final edited form as:

Exp Mol Pathol. 2021 April ; 119: 104605. doi:10.1016/j.yexmp.2021.104605.

Mass Spectrometry Imaging of Blast Overpressure Induced Modulation of GABA/Glutamate Levels in the Central Auditory Neuraxis of Chinchilla

Kevin Zemaitis[1], **Kathiravan Kaliyappan**[2], **Valarie Freirichs**[1], **Alan Friedman**[3], **Vijaya Prakash Krishnan Muthaiah**[2]

[1]Department of Chemistry, Natural Sciences Complex, University at Buffalo, State University of New York, Buffalo, NY 14260.

[2]Department of Rehabilitation Sciences, Kimball Tower, University at Buffalo, State University of New York, Buffalo, NY 14215.

[3]Department of Materials Design and Innovation, School of Engineering and Applied Sciences, University at Buffalo, State University of New York, Buffalo, NY 14260

Abstract

Acoustic trauma damages inner ear neural structures including cochlear hair cells which result in hearing loss and neurotransmitter imbalances within the synapses of the central auditory pathway. Disruption of GABA/glutamate levels underlies, tinnitus, a phantom perception of sound that persists post-exposure to blast noise which may manifest in tandem with acute/chronic loss of hearing. Many putative theories explain tinnitus physiology based on indirect and direct assays in animal models and humans, although there is no comprehensive evidence to explain the phenomenon. Here, GABA/glutamate levels were imaged and quantified in a blast overpressure model of chinchillas using Fourier transform ion cyclotron mass spectrometry. The direct measurement from whole-brain section identified the relative levels of GABA/glutamate in the central auditory neuraxis centers including the cochlear nucleus, inferior colliculus and auditory cortex. These preliminary results provide insight on the homeostasis of GABA/glutamate within whole-brain sections of chinchilla for investigation of the pathomechanism of blast-induced tinnitus.

GRAPHICAL ABSTRACT:

Corresponding Author: Vijaya Prakash Krishnan Muthaiah, PT, PhD, Assistant Professor, Department of Rehabilitation Sciences, School of Public Health and Health Sciences, University at Buffalo, Buffalo, NY 14215, USA. vijayapr@buffalo.edu.

Author Statement:

Vijaya Prakash Krishnan Muthaiah conceptualized the study, supervised, administered the project, provided the resources, and prepared the manuscript. Kevin Zemaitis processed the brain sections, acquired and analyzed the mass spectrometry data, and prepared the manuscript. Kathiravan Kaliyappan completed the blast exposure, histological sectioning, and edited the manuscript. Valerie Frerichs and Alan Friedman administered the mass spectrometry experiments and data acquisition, reviewed, and edited the portions of the manuscript related to those assays.

Declaration of interest:

None.

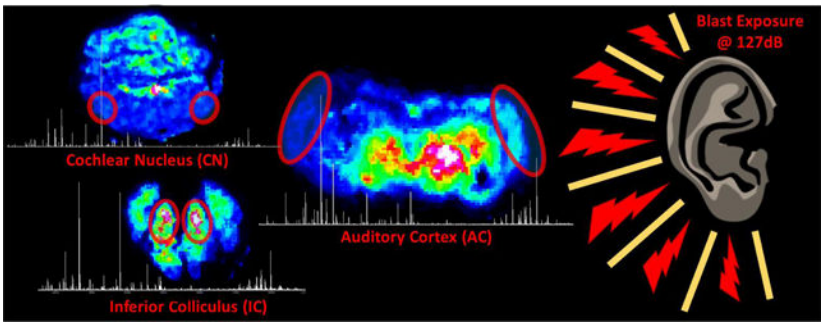

Keywords

GABA/Glutamate homeostasis; blast exposure; blast overpressure; chinchilla; tinnitus; mass spectrometry imaging

INTRODUCTION:

Tinnitus is a phantom sensation of sound in the absence of an external auditory stimulus, and is the most prevalent military related service disability. Approximately 75% of service members' combat injuries result from blast exposures (Gordon et al., 2017; Karch et al., 2016), with 20% of veteran's reporting tinnitus (Veterans Benefits Administration Annual Report, 2016). Tinnitus usually occurs in conjunction with hearing loss, although not infrequently is reported in those with normal hearing. With exposure to damaging levels of sound, known as blast overpressure (BOP) injuring cochlear hair cells and afferent synapses, causing hearing loss. Several theories, and some empirical data, suggest that a reduction in peripheral auditory nerve input to the brainstem following acoustic trauma can lead to tinnitus. However, to date, there is no compelling experimental evidence that peripheral deafferentation (now popularly known as cochlear synaptopathy) causes tinnitus.

The auditory pathway starts with simulation of the auditory cortex (AC), where multiple feedback loops exist between the midbrain components of the auditory neuraxis, the cochlear nucleus (CN) and inferior colliculus (IC) (Huffman and Henson, 1990; Markovitz et al., 2013; Schofield and Beebe, 2019). Ultra-fast highly reliable synaptic responses are essential for normal auditory temporal processing. Among the neurotransmitter systems known to regulate auditory processing including amino acids, monoamines, and peptides; amino acid neurotransmitters glutamate and gamma-aminobutyric acid (GABA) are attributed to normal excitatory and inhibitory auditory processing respectively (Yang et al., 2011). Hearing loss reportedly increases excitability, perhaps due to diminished inhibition in the central auditory system (Kotak et al., 2005; Salvi et al., 2000). This alters the central synaptic processing including alterations of synaptic strength, neuronal excitability and kinetic properties, thereby altering the central auditory neural activity. Evidence indicates reduced GABAergic inhibition in the dorsal CN (Middleton et al., 2011). and AC (Llano et al., 2012) of noise trauma tinnitus animal models, and GABA receptor affinity is found to be reduced in the IC following salicylate exposure (Bauer et al., 2000). The inter-individual variation of auditory multi-stability has been linked to the balance of excitatory glutamatergic and inhibitory GABAergic signaling between different

brain regions (Kondo et al., 2017). Thus, loss of excitation and inhibition balance results in altered neural activity such as spontaneous hyperactivity, increased burst firing, heightened neural synchrony, aberrant tonotopic maps, shift in frequency receptive fields, as well as an abnormal coupling in distributed neural networks of auditory and non-auditory structures in sub-cortical regions.

Our existing knowledge on neurotransmitters of the auditory system was obtained through indirect assays such as receptor density measurements, and quantification of enzymes involved in neurotransmitter synthesis (Caspary et al., 2013; Wu et al., 2018). With several direct, invasive strategies having been adopted in animal models using ex-vivo high-performance liquid chromatography (HPLC), in-vivo fast scanning cyclic voltammetry (FSCV), microdialysis, or nano-gap electrodes which have chemical specificity but are not capable of global analysis (Komoto et al., 2020). Recently, auditory neurochemistry has been studied in humans and rats using non-invasive magnetic resonance spectroscopy (MRS) (Brozoski and Odintsov, 2012). Using MRS, reduced GABA concentration in the central auditory system has been reported in tinnitus patients indicating reduced GABAergic inhibition and therefore a relative excess of excitation in the auditory system (Sedley et al., 2015). However the direct link from animal model of noise-induced tinnitus to human pathophysiological response is not perfect with many murine species, and guinea pig having been investigated (Brozoski and Bauer, 2016). Chinchillas however are unique due to their similarity to human hearing frequencies and transmission of sound through the ear (Miller, 1970; Peacock et al., 2018). As well as similar anatomical size chinchilla allow for closer relation to humans due to similar conductance through the physical ear (Ravicz and Rosowski, 2012). In the present study, we detected levels of GABA and glutamate changes along with other biomolecules in fresh chinchilla brain sections containing the CN, IC and AC regions using matrix- assisted laser desorption/ ionization (MALDI) Fourier transform ion cyclotron resonance mass spectrometry imaging (FT-ICR MSI).

MSI has seen widespread use in translational research and clinical laboratories largely due to the label-free, simultaneous detection of many classes of molecules (Norris and Caprioli, 2013). In MSI, analytes are desorbed and ionized directly from a sampled surface and subsequently detected according to mass-to-charge ratios (*m/z*). After creation, ions are trapped within the detection cell by applied electric potentials within a high magnetic field and are excited to a sustained orbit (Nikolaev et al., 2016). The ions periodic motion in this cell is the cyclotron frequency, which depends on the ratio of *m/z* and strength of the magnetic field. The ions are detected as an image current on a pair of opposing electrode plates, which is ultimately converted to a mass spectrum through Fourier transform. FT-ICR and similar mass analyzers achieve the highest mass resolving powers in mass spectrometry with an accuracy of around 1 ppm or less (Kaiser et al., 2011). When combined with MALDI and other ionization sources capable of imaging, such as secondary ion mass spectrometry (SIMS), and desorption electrospray ionization (DESI), mass spectrometry preserves the spatial distribution of detected biomolecules in tissue producing pixelated chemical images corresponding to intensities of selected molecules within the mass spectrum (Caprioli et al., 1997; Todd et al., 2001; Wiseman et al., 2006). Combining the high chemical specificity of in-vivo methods, and the sensitivity of mass spectrometry with the visualization possible by microscopy —allowing for the

direct mapping of lipids, peptides and proteins, and small molecules throughout sections of tissue by MSI (Buchberger et al., 2018). With recent developments in sample preparation and procedures, MALDI-MSI has been applied to animal models of disease and trauma for profiling of amine-containing neurotransmitters, which usually have poor ionization efficiencies and are suppressed by isobaric matrix clusters (Gemperline et al., 2014). Herein reported is an adopted technique for MALDI-MSI (Esteve et al., 2016; Shariatgorji et al., 2019; Shariatgorji et al., 2014; Shariatgorji et al., 2015), which allowed for the relative quantification of neurotransmitters through derivatization utilizing pyrylium salts in the neuroaxis centers (CN, IC and AC) of the primary auditory pathway of chinchilla following exposure to blast overpressure.

MATERIALS AND METHODS:

Chemicals

α-cyano-4-hydroxycinnamic acid (CHCA, 99%), 2,4-diphenyl-6-methylpyrylium tetrafluoroborate (DPMP-TFB), and methanol (HPLC grade) were obtained from Sigma Aldrich (St. Louis, MO), optimal cutting temperature compound (OCT) was obtained from Fisher Healthcare (Houston, TX), nanopure water was obtained from a ThermoScientific Barnstead Nanopure system (Dubuque, IA). Ketamine was from Vedco (St. Joseph, MO), xylazine was from Akorn Animal Health (Lake Forest, IL), and fatal plus was obtained from Vortech Pharmaceuticals (Dearborn, MI).

Blast Overpressure (BOP) Exposure:

All experiments were performed according to protocols approved by the University at Buffalo's Institutional Animal Care and Use Committee protocol number 201800131. Adult male chinchillas (n=1) approximately 4–6 months old were used for this study. Prior to blast overpressure (BOP) exposure the chinchilla was anesthetized with ketamine (40 mg/kg, intraperitoneal) and xylazine (4 mg/kg, subcutaneous). Anesthetized chinchillas were exposed to a unilateral impulse (Left side, ipsilateral) generated by an acoustic shock tube similar to the one designed and developed by the National Institute for Occupational Safety and Health (NIOSH) by placing them at a calibrated distance from the outer horn of the tube. This shock tube meets the operational requirements based on ANSI/ASA S12.42–2010 standard to test hearing protection devices from impulse noise and is similar to the one used by (Hickman et al., 2018)'s study of blast-induced cochlear dysfunction in chinchillas. The shock tube is fitted with a compressed airflow system, pressure chamber and catenoid horn. The shock tube is capable of generating impulse noise up to 40 psi (275 kPa) with its energy greatest below several kHz in the frequency spectrum of acoustic energy (Figure 1). In this study, BOP was at 172 dB SPL when the pressure chamber is set at 23 psi. The impulse waveform from our set-up whose initial acoustic overpressure is less than 2 milliseconds (Figure 2). The acoustic sound pressure data was collected through a B&K ¼-inch pressure field microphone (Type 4938).

Tissue Processing:

The animals were euthanized at the end of the study period (post-BOP 3 days) by injecting a euthanizing dose (1mL/10lbs) of fatal plus solution (pentobarbital sodium) and fresh

brains were harvested immediately without perfusion, flash-frozen, and embedded in OCT compound before sectioning. The sections of the central auditory neuraxis center (CN, IC, and AC) were taken at 15 μm using a Leica CM3050S cryostat (Leica Biosystems Inc, USA) at −25 °C. The sections were thaw mounted onto indium tin oxide coated slides from Bruker Daltronics (Billerica, MA, USA) for MSI and stored at −80 °C until further analysis.

Sample Preparation:

Neurotransmitter derivatization and imaging in coronal sections of the chinchilla brain was performed by adopting the methods of (Shariatgorji et al., 2014; Shariatgorji et al., 2015). The MSI of neurotransmitters was developed using on-tissue derivatization using a pyrylium salt before matrix deposition. Briefly, a 2.0 mg/mL solution of 2,4-diphenyl-6-methylpyrylium tetrafluoroborate (DPMP-TFB) in methanol: water (1:1) was applied directly onto tissue using a Bruker Daltronic ImagePrep pneumatic sprayer (Bremen, Germany). The derivatization agent was allowed to react at ambient temperature as reported (Esteve et al., 2016) and exposed to methanolic vapor and acidification of the tissue as reported by (Shariatgorji et al., 2014). Post derivatization, an in-house sublimation chamber was used to apply the matrix to the tissue. Two slides at a time were sublimed with α-cyano-4-hydroxycinnamic (CHCA) acid at a temperature of 180 °C. Sublimation was allowed to persist for 20 minutes, with pressure stabilizing at 140 mTorr. The sample was desiccated before weighing and measurement of the area sublimed for determination of coverage, with an average coverage of 128 μg/cm^2.

MALDI FT-ICR MSI:

MSI was carried out on a 12T Bruker Daltronics SolariX FT-ICR MS equipped with a dual electrospray and MALDI source with a 1kHz SmartBeam II frequency-tripled Nd:YAG laser (Bremen, Germany). A digitally scanned image was loaded into FlexImaging 5.0 and samples were analyzed at 225 μm spatial resolution in the positive ionization mode with laser conditions optimized at 1000 laser shots per pixel at a rate of 1 kHz. Broadband excitation was used to detect from *m/z* 98.3 to 1000.0 with a time-domain of 2M for a transient of 0.5592 s. Images produced from FlexImaging 5.0 and SCiLS Lab (build 2019b) were normalized against the root mean square of all data points. With total signal from each hemisphere processed as a region of interest and averaged into DataAnalysis 5.0 for further processing.

RESULTS AND DISCUSSION:

In this preliminary study, the AC as well as midbrain components of the auditory pathway (IC and CN) were profiled as shown in Figure 3, with stereotaxic regions highlighted in cresyl-fast violet (CFV) brain coronal sections of the CN, IC and AC. Analysis specifically targeted excitatory and inhibitory neurotransmitters within a chinchilla model of BOP induced tinnitus. The derivatization technique was able to enhance the ionization of the small endogenous amines and for DPMP-TFB derivatives resulting in a monoisotopic mass shift of 229.10173 ($C_{18}H_{13}$) for compounds, with GABA being the most intense derivative detected. Not all pyrylium derivatives of neurotransmitters form identically, as previously noted in comparative derivatization studies (Shariatgorji et al., 2015), and with DPMP-TFB

molecular ions of monoamine neurotransmitter derivatives were not detected. Represented in Figure 4 are the intensity maps produced from the molecular ion of derivatized GABA at *m/z* 332.1646 (−0.3ppm error), and was confirmed through analysis of in-solution derivatization products and on-tissue tandem mass spectrometry shown in Supplementary Figure S1. Shown in Supplementary Figures S2, S3, and S4 are the corresponding images produced from phospholipid signals from each of the sections. Changes within the profiles from control to BOP exposed tissue was not seen within the chemical images 3 days post-BOP, however concentration of potassium and sodium were altered based upon distributions of lipid signal.

Unilaterally deafened animals have previously displayed increased sound-evoked activity in the ipsilateral IC and AC, likely attributable to a change in the balance between existing excitatory and inhibitory inputs (Mossop et al., 2000). With presynaptic NR2B-containing NMDA receptors having been shown to enhance glutamate release (Berretta and Jones, 1996). Within the AC section of the BOP exposed tissue, a hemispherical variance is observed (Figure 4D) and seen within plots of averaged signal intensity within the hemisphere with a relative depletion of GABA unilaterally in the averaged intensities within the left hemisphere of the BOP exposed animal (Figure 5). This does average auditory and non-auditory area of the hemisphere however the GABA intensity in the AC is found to be decreased in the ipsilateral hemisphere (Figure 4D, BOP exposed side) when compared to the contralateral hemisphere of mid-AC section (Figure 4A). All control sections control sections were observed with no distinct unilateral variances for GABA (Figure 4A, 4B, 4C), and confirmed in the plots of averaged intensities (Figure 5). In the AC of tinnitus subjects, reduction in GABA has been observed using magnetic resonance spectroscopy (MRS) (Brozoski and Odintsov, 2012; Sedley et al., 2015). Yasen and colleagues have also determined the traumatic brain injury-induced region-specific changes of GABA and glutamate in the primary motor cortex and dorsolateral prefrontal cortex using MRS (Yasen et al., 2018).

Although other unilateral events are not observed for GABA within the CN or IC sections of the BOP exposed brain, a global depletion within the IC is observed when compared to the control. Finding that GABA intensity is decreased in the BOP exposed mid-IC section (Figure 4F) when compared to control of the mid-IC section (Figure 4C). Prior electrophysiological analysis has demonstrated that elevated bursting occurs alongside lower variance within a subset of neurons within the IC in chinchillas with tinnitus. With a pathophysiological cause of deafferation in the shell of the IC, rather than direct afferent impact upon the synapsis after tinnitus (Bauer et al., 2008). With traumatic brain injury-induced acute and chronic changes of GABA/glutamate homeostasis in the brain having been previously reviewed (Guerriero et al., 2015). Electrophysiological evidence from animal studies and non-invasive neurotransmitter estimation in humans indicates that BOP induces tinnitus, and alters sensory processing in the brain due to cortical and subcortical abnormalities of GABA inhibition which includes both auditory and non-auditory cortical areas (Mao et al., 2012; Ouyang et al., 2017). Within the cerebellum, no such unilateral or bilateral depletion is noted for GABA with the control (Figure 4B) and BOP exposed tissues (Figure 4E) having consistent signal in the total averaged from hemispheres in the CN (Figure 5).

The extracted relative intensity ratio (R/L) was investigated for the total averaged signal, with enhancement within the sections containing the AC, also confirming the unilateral variance visually seen within the signal of GABA in the BOP exposed brain and the global decrease of GABA levels in the BOP exposed sections containing the IC (Figure 5), with minor variation to the peak intensity ratio (R/L). Whereas glutamate is observed without distinct changes in the ratio between the right and left hemispheres for all samples (Figure 5). High contrast images with lateral biases were also not seen within either control or BOP exposed sections for glutamate, with consistent signal in each hemisphere in the AC, CN, and IC as seen within the plots of averaged intensities (Figure 5). This hemispherical segmentation does not directly compare solely the auditory regions, but total levels in the section. With regions of interest profiled from visual inspection of the chemical images. Further analysis with higher spatial resolution will be needed to completely segment the subsections of the auditory pathway, and is the primary reasons why sub-regions were not segmented. This is where the preservation and identification through spatial distributions are key.

One prominent theory is that following deprivation of peripheral sensory input, the brain fails to adapt properly causing a pathological increase in aberrant neural activity such as spontaneous hyperactivity, increased burst firing, heightened neural synchrony, modified tonotopic maps, shift in frequency receptive fields, as well as an abnormal coupling in distributed neural networks of auditory and non-auditory structures in subcortical regions (Eggermont, 2016; Lockwood et al., 2002). Also that following reduced auditory-nerve activity after acoustic trauma, an abnormal central compensation is first triggered at the level of the brainstem and then distributes the altered activity patterns to more rostral auditory nuclei (Henry et al., 2014; Moller et al., 2015). Information transmission along the auditory nerve is compromised and centrally compensated following sound-induced trauma. Irrespective of the nature of the insult, cortical gain enhancement is a plausible mechanism of tinnitus (Auerbach et al., 2014), and neurotransmitter modulation is considered a feasible pathomechanism of tinnitus (Sun et al., 2007). Despite the electrophysiological evidence of cortical abnormalities in tinnitus, the changes in the neurotransmitter chemistry following BOP have not been investigated. Quantitative analysis of neurotransmitters in the brain, specifically GABA and glutamate, will be helpful to understand BOP induced neurotransmitter modulation and region-specific changes in both auditory and non-auditory areas. With few experimental studies having quantified specific BOP induced neurotransmitters changes using HPLC (Cui et al., 2012; Kawa et al., 2015). Utilizing methodologies such as MSI becomes beneficial over electrophysiology and other techniques due to the preservation of spatial distributions relative to set spatial resolutions. Allowing for the ability to globally profile all neurochemical changes within sub-regions. Demonstrated here was a targeted approach for GABA and glutamate, with recent literature providing a more comprehensive mapping of neurotransmitters.

CONCLUSION:

In the present study, we developed a method to relatively quantify levels of the neurotransmitters GABA and glutamate within the CN, IC and AC of fresh chinchilla brain sections using MALDI FT-ICR MSI. Detection of neurotransmitters in various

regions of the auditory pathway in BOP exposed chinchillas enabled us to demonstrate region-specific BOP induced imbalance in the excitation-inhibition network in various brain regions. Estimation of relative neurotransmitter levels using MSI allowed us to quantify neurotransmitters for an entire brain section in experimental animal models, instead of quantifying changes in specific stereotaxic coordinates using other techniques such as HPLC, FSCV, or in-vivo microdialysis. Further, in addition to whole hemisphere quantification, the study of neurotransmitter modulation can be confined to specific anatomical regions guided by correlating the high contrast MSI images with concurrent cresyl-fast violet histological sections. Thus, this workflow allows for the estimation of neurotransmitter modulation to be correlated with morphological changes. Our preliminary study by MSI in the CN, IC and AC indicated that BOP disrupts GABA levels, resulting in a unilateral variance of GABA in the AC and global depletion of GABA in the IC. Our results of AC and IC GABA depletion in BOP exposed chinchilla is inconsonant with evidence of GABA reduction using electrophysiology and non-invasive measures in humans and rats. However, further studies are warranted to increase the power of the analysis, but for the first time MALDI-MSI was used for mapping the auditory pathway in a BOP exposure model of tinnitus in chinchillas, providing critical insights on the unknown pathomechanism of neurotransmitter modulation through direct analysis of blast-induced tinnitus throughout the sections of the central auditory neuraxis.

Supplementary Material

Refer to Web version on PubMed Central for supplementary material.

Acknowledgements:

We acknowledge the funding through the National Institutes of Health through the National Center for Research Resources (Grant S10-RR029517-01) used to obtain the 12T Bruker SolariX FT-ICR MS used within the study and the Chemistry Instrument Center at the University at Buffalo for housing the mass spectrometer, and Hearing Health Foundation for providing financial support for the corresponding author. We also would like to acknowledge Prof. Robert F Burkard for critically reading this manuscript.

References

Auerbach BD, et al. , 2014. Central Gain Control in Tinnitus and Hyperacusis. Frontiers in Neurology. 5.

Bauer CA, et al. , 2000. Effects of chronic salicylate on GABAergic activity in rat inferior colliculus. Hearing Research. 147, 175–182. [PubMed: 10962183]

Bauer CA, et al. , 2008. Tinnitus and inferior colliculus activity in chinchillas related to three distinct patterns of cochlear trauma. J Neurosci Res. 86, 2564–78. [PubMed: 18438941]

Berretta N, Jones RS, 1996. Tonic facilitation of glutamate release by presynaptic N-methyl-D-aspartate autoreceptors in the entorhinal cortex. Neuroscience. 75, 339–44. [PubMed: 8931000]

Brozoski T, Odintsov B, 2012. Gamma-aminobutyric acid and glutamic acid levels in the auditory pathway of rats with chronic tinnitus: a direct determination using high resolution point-resolved proton magnetic resonance spectroscopy (1H-MRS). Frontiers in Systems Neuroscience. 6.

Brozoski TJ, Bauer CA, 2016. Animal models of tinnitus. Hearing Research. 338, 88–97. [PubMed: 26520585]

Buchberger AR, et al. , 2018. Mass Spectrometry Imaging: A Review of Emerging Advancements and Future Insights. Analytical chemistry. 90, 240–265. [PubMed: 29155564]

Caprioli RM, et al. , 1997. Molecular imaging of biological samples: localization of peptides and proteins using MALDI-TOF MS. Anal Chem. 69, 4751–60. [PubMed: 9406525]

Caspary DM, et al. , 2013. Age-related GABAA receptor changes in rat auditory cortex. Neurobiol Aging. 34, 1486–96. [PubMed: 23257264]

Cui B, et al. , 2012. Impulse noise exposure in rats causes cognitive deficits and changes in hippocampal neurotransmitter signaling and tau phosphorylation. Brain Res. 1427, 35–43. [PubMed: 22055774]

Eggermont JJ, 2016. Can Animal Models Contribute to Understanding Tinnitus Heterogeneity in Humans? Frontiers in Aging Neuroscience. 8.

Esteve C, et al. , 2016. Mass spectrometry imaging of amino neurotransmitters: a comparison of derivatization methods and application in mouse brain tissue. Metabolomics : Official journal of the Metabolomic Society. 12, 30–30. [PubMed: 26793043]

Gemperline E, et al. , 2014. Challenges and recent advances in mass spectrometric imaging of neurotransmitters. Bioanalysis. 6, 525–540. [PubMed: 24568355]

Gordon JS, et al. , 2017. Audiologic characteristics in a sample of recently-separated military Veterans: The Noise Outcomes in Servicemembers Epidemiology Study (NOISE Study). Hear Res. 349, 21–30. [PubMed: 27913314]

Guerriero RM, et al. , 2015. Glutamate and GABA imbalance following traumatic brain injury. Curr Neurol Neurosci Rep. 15, 27. [PubMed: 25796572]

Henry JA, et al. , 2014. Underlying mechanisms of tinnitus: review and clinical implications. Journal of the American Academy of Audiology. 25, 5–126. [PubMed: 24622858]

Hickman TT, et al. , 2018. Blast-induced cochlear synaptopathy in chinchillas. Scientific Reports. 8, 10740.

Huffman RF, Henson OW Jr., 1990. The descending auditory pathway and acousticomotor systems: connections with the inferior colliculus. Brain Res Brain Res Rev. 15, 295–323. [PubMed: 2289088]

Kaiser NK, et al. , 2011. A Novel 9.4 Tesla FTICR Mass Spectrometer with Improved Sensitivity, Mass Resolution, and Mass Range. Journal of The American Society for Mass Spectrometry. 22, 1343–1351. [PubMed: 21953188]

Karch SJ, et al. , 2016. Hearing Loss and Tinnitus in Military Personnel with Deployment-Related Mild Traumatic Brain Injury. US Army Med Dep J. 52–63.

Kawa L, et al. , 2015. Neurotransmitter Systems in a Mild Blast Traumatic Brain Injury Model: Catecholamines and Serotonin. Journal of neurotrauma. 32, 1190–1199. [PubMed: 25525686]

Komoto Y, et al. , 2020. Time-resolved neurotransmitter detection in mouse brain tissue using an artificial intelligence-nanogap. Scientific Reports. 10, 11244.

Kondo HM, et al. , 2017. Auditory multistability and neurotransmitter concentrations in the human brain. Philosophical transactions of the Royal Society of London. Series B, Biological sciences. 372, 20160110.

Kotak VC, et al. , 2005. Hearing loss raises excitability in the auditory cortex. J Neurosci. 25, 3908–18. [PubMed: 15829643]

Llano DA, et al. , 2012. Diminished cortical inhibition in an aging mouse model of chronic tinnitus. J Neurosci. 32, 16141–8. [PubMed: 23152598]

Lockwood AH, et al. , 2002. Tinnitus. N Engl J Med. 347, 904–10. [PubMed: 12239260]

Mao JC, et al. , 2012. Blast-induced tinnitus and hearing loss in rats: behavioral and imaging assays. Journal of neurotrauma. 29, 430–444. [PubMed: 21933015]

Markovitz C, et al. , 2013. Tonotopic and localized pathways from primary auditory cortex to the central nucleus of the inferior colliculus. Frontiers in Neural Circuits. 7.

Middleton JW, et al. , 2011. Mice with behavioral evidence of tinnitus exhibit dorsal cochlear nucleus hyperactivity because of decreased GABAergic inhibition. Proceedings of the National Academy of Sciences. 108, 7601–7606.

Miller JD, 1970. Audibility curve of the chinchilla. J Acoust Soc Am. 48, 513–23. [PubMed: 5470498]

Moller AR, et al. , 2015. Pathology of Tinnitus and Hyperacusis-Clinical Implications. Biomed Res Int. 2015, 608437.

Mossop JE, et al. , 2000. Down-regulation of inhibition following unilateral deafening. Hear Res. 147, 183–7. [PubMed: 10962184]

Nikolaev EN, et al. , 2016. Fourier transform ion cyclotron resonance (FT ICR) mass spectrometry: Theory and simulations. Mass Spectrom Rev. 35, 219–58. [PubMed: 24515872]

Norris JL, Caprioli RM, 2013. Analysis of Tissue Specimens by Matrix-Assisted Laser Desorption/Ionization Imaging Mass Spectrometry in Biological and Clinical Research. Chemical Reviews. 113, 2309–2342. [PubMed: 23394164]

Ouyang J, et al. , 2017. Blast-Induced Tinnitus and Elevated Central Auditory and Limbic Activity in Rats: A Manganese-Enhanced MRI and Behavioral Study. Scientific Reports. 7, 4852. [PubMed: 28687812]

Peacock J, et al. , 2018. Intracochlear pressure in response to high intensity, low frequency sounds in chinchilla. Hear Res. 367, 213–222. [PubMed: 29945804]

Ravicz ME, Rosowski JJ, 2012. Chinchilla middle-ear admittance and sound power: high-frequency estimates and effects of inner-ear modifications. The Journal of the Acoustical Society of America. 132, 2437–2454. [PubMed: 23039439]

Salvi RJ, et al. , 2000. Auditory plasticity and hyperactivity following cochlear damage. Hear Res. 147, 261–74. [PubMed: 10962190]

Schofield BR, Beebe NL, Descending Auditory Pathways and Plasticity. Oxford University Press, 2019.

Sedley W, et al. , 2015. Human Auditory Cortex Neurochemistry Reflects the Presence and Severity of Tinnitus. The Journal of Neuroscience. 35, 14822–14828. [PubMed: 26538652]

Shariatgorji M, et al. , 2019. Comprehensive mapping of neurotransmitter networks by MALDI–MS imaging. Nature Methods. 16, 1021–1028. [PubMed: 31548706]

Shariatgorji M, et al. , 2014. Direct Targeted Quantitative Molecular Imaging of Neurotransmitters in Brain Tissue Sections. Neuron. 84, 697–707. [PubMed: 25453841]

Shariatgorji M, et al. , 2015. Pyrylium Salts as Reactive Matrices for MALDI-MS Imaging of Biologically Active Primary Amines. Journal of The American Society for Mass Spectrometry. 26, 934–939. [PubMed: 25821050]

Sun W, et al. , 2007. Neurotransmitter Modulation Relates with Tinnitus Signal Generation and Management. Journal of Otology. 2, 63–69.

Todd PJ, et al. , 2001. Organic ion imaging of biological tissue with secondary ion mass spectrometry and matrix-assisted laser desorption/ionization. Journal of Mass Spectrometry. 36, 355–369. [PubMed: 11333438]

Wiseman JM, et al. , 2006. Tissue Imaging at Atmospheric Pressure Using Desorption Electrospray Ionization (DESI) Mass Spectrometry. Angewandte Chemie International Edition. 45, 7188–7192. [PubMed: 17001721]

Wu C, et al. , 2018. Changes in GABA and glutamate receptors on auditory cortical excitatory neurons in a rat model of salicylate-induced tinnitus. American journal of translational research. 10, 3941–3955. [PubMed: 30662641]

Yang Y-M, et al. , 2011. GluA4 is indispensable for driving fast neurotransmission across a high-fidelity central synapse. The Journal of physiology. 589, 4209–4227. [PubMed: 21690196]

Yasen AL, et al. , 2018. Glutamate and GABA concentrations following mild traumatic brain injury: a pilot study. J Neurophysiol. 120, 1318–1322. [PubMed: 29924705]

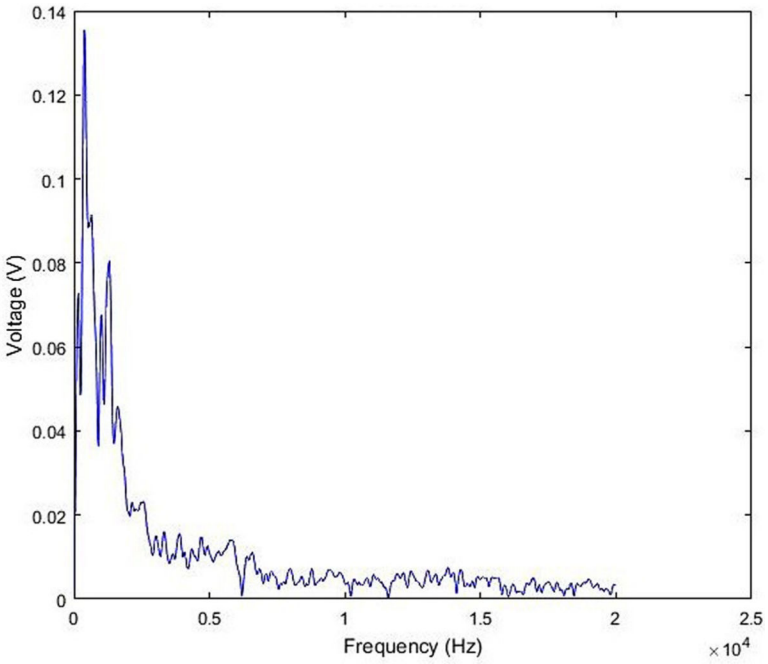

Fig. 1.

Frequency spectrum of acoustic energy in the blast overpressure (BOP) exposure used within this study.

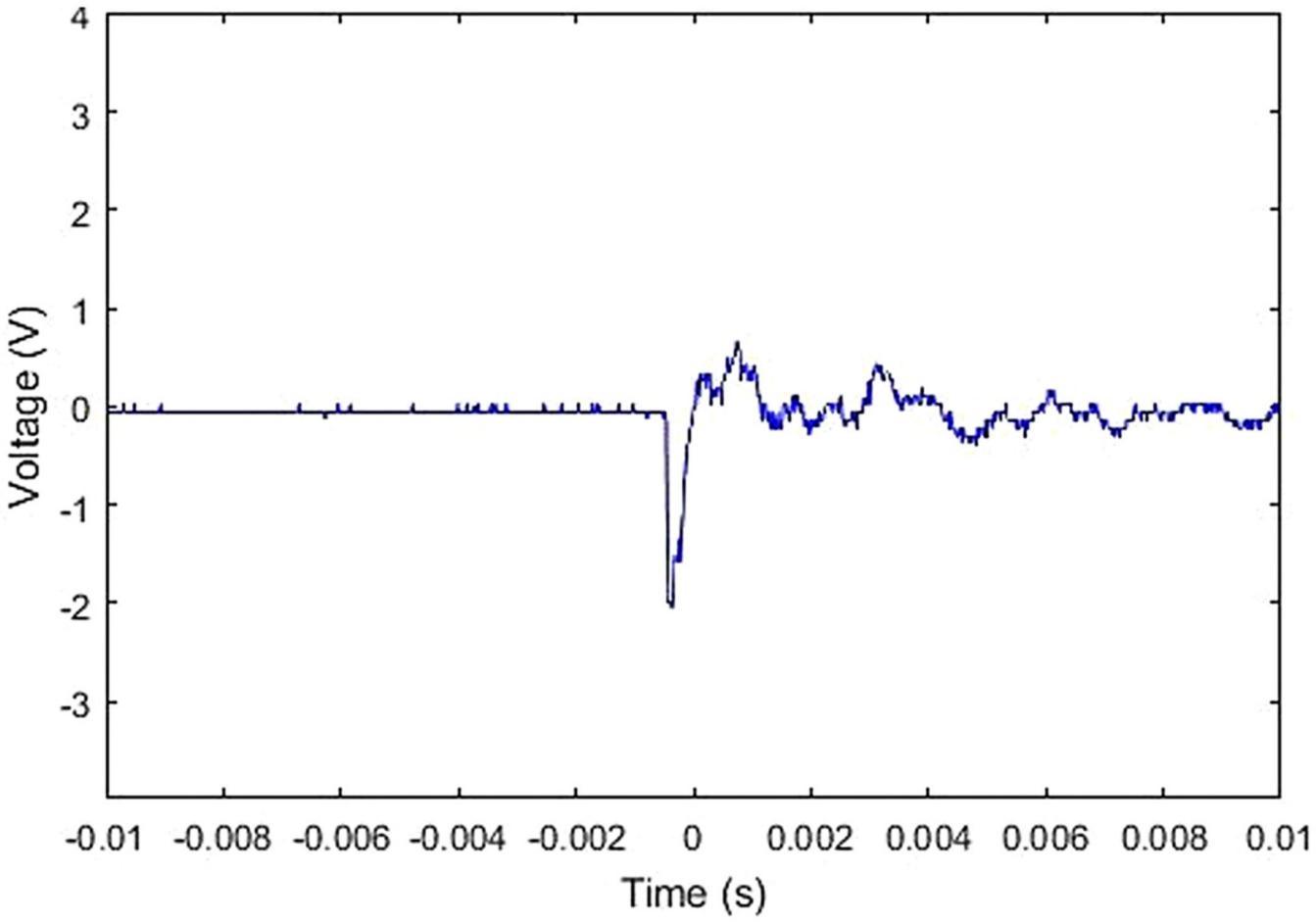

Fig. 2.

The impulse waveform of blast overpressure (BOP) exposure used in the unilateral acoustic insult of the left ear of the chinchilla.

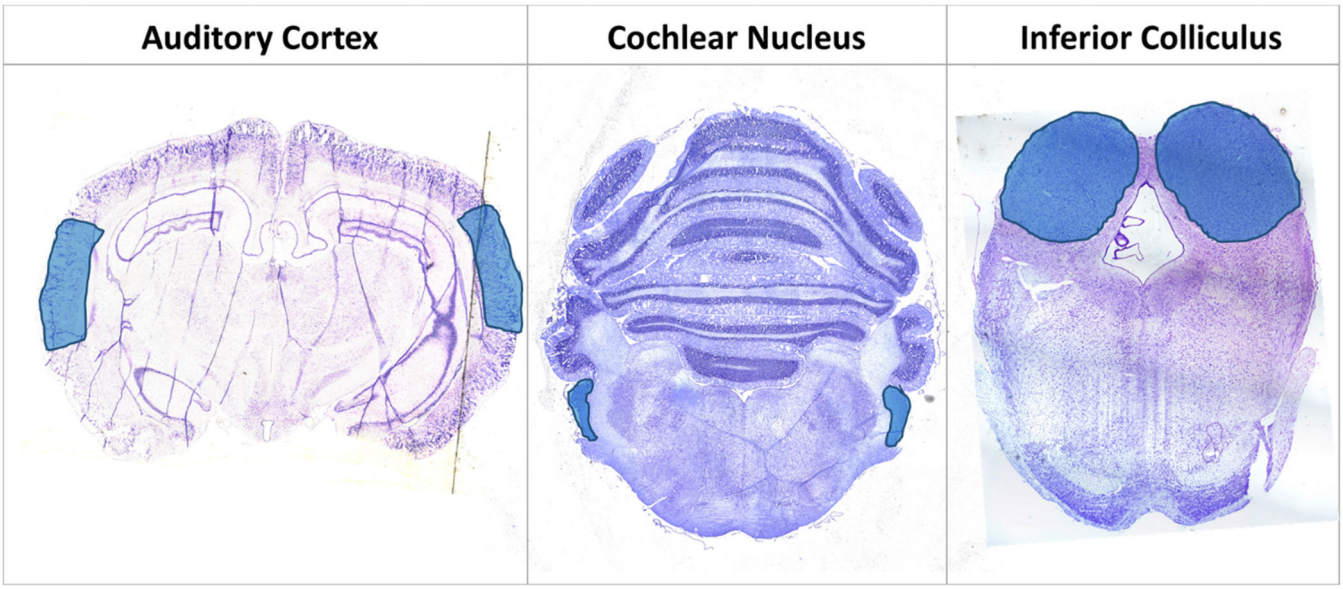

Fig. 3.

Cresyl-fast violet (CFV) stained 15 μm sections from the three areas of the primary central neuraxis within the sectioned slices of the male chinchilla brain. The blue areas are highlighting the auditory cortex (AC), cochlear nucleus (CN), and inferior colliculus (IC) regions of interest. (For interpretation of the references to colour in this figure legend, the reader is referred to the web version of this article.)

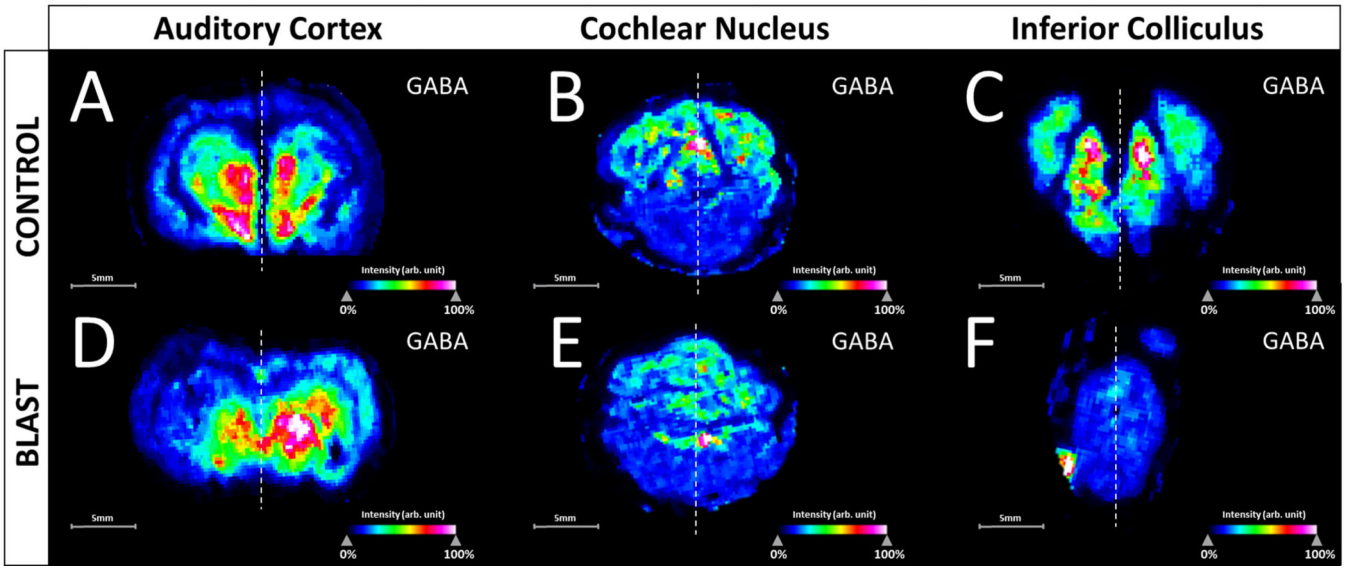

Fig. 4.

Root mean square (RMS) normalized intensity maps of the molecular ion of GABA derivitized with DPMP within the three neuraxis centers. Sections from the control animal are highlighted in the top row, with sections from the blast-overpressure (BOP) animal in the bottom row. A and D are coronal sections containing the primary auditory cortex (AC), B and E are coronal sections within the cerebellum containing the cochlear nucleus (CN), and C and F are caudal sections of the brain containing the mid inferior colliculus (IC). Control and blast images were processed in SCiLS Lab (build 2019b) for each neuraxis center simultaneously. Dotted line represents the segmentation of ipsilateral and contralateral hemispheres.

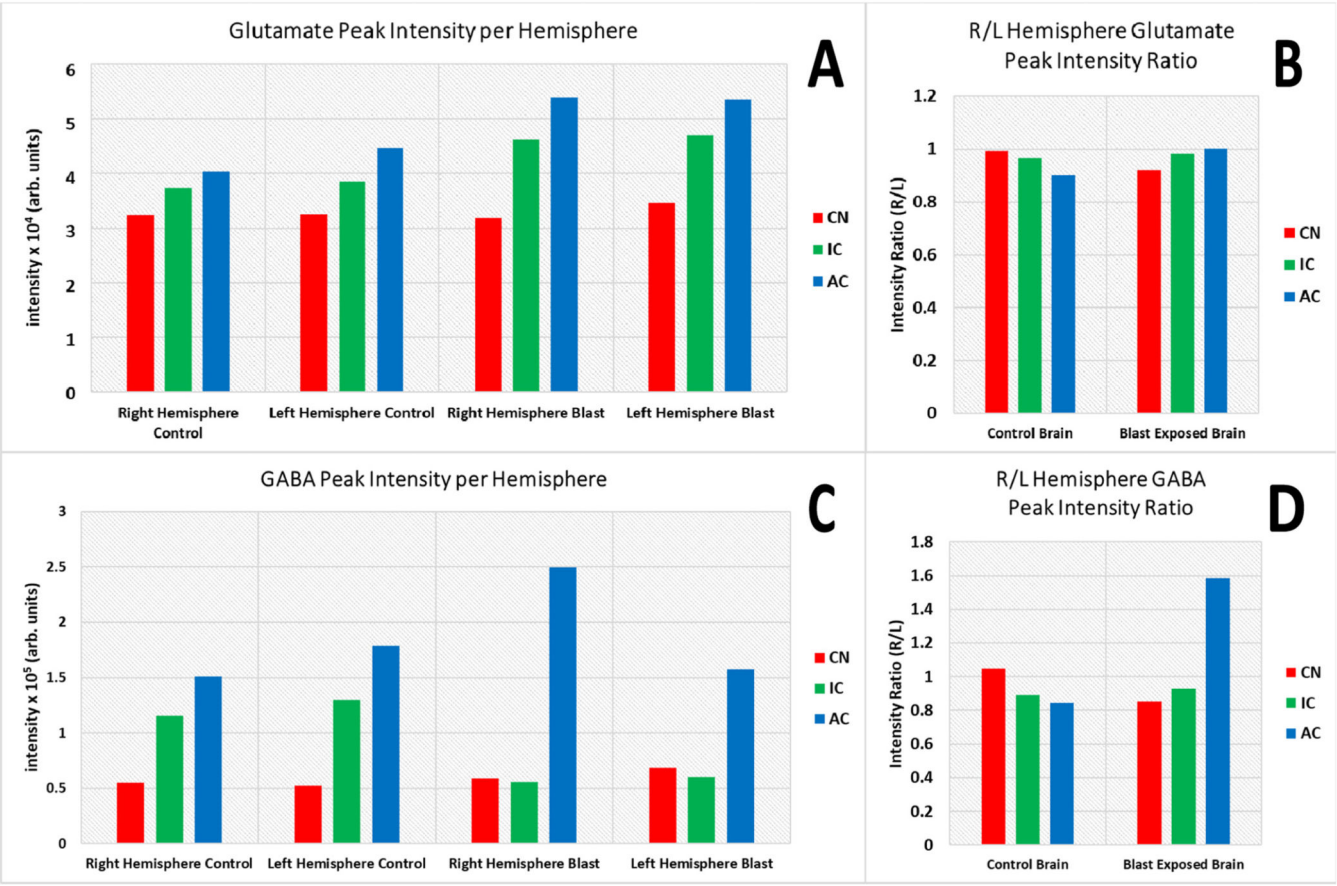

Fig. 5.

Plot of the summed intensities of a putative glutamate ion (A) and GABA (B) from within the left and right hemispheres of blast and control brain sections (n = 1) processed from FlexImaging 5.0 into DataAnalysis 5.0. C, and D represent the average ratios of the summed intensities from the of the right/left hemibrain. Red bars correspond to the summed intensity from the cerebellar hemispheres containing the cochlear nucleus (CN), green bars correspond to the inferior colliculus (IC), and blue bars correspond to the primary auditory cortex (AC). (For interpretation of the references to colour in this figure legend, the reader is referred to the web version of this article.)